ACS APPLIED BIO MATERIALS

www.acsabm.org Article

Cu(I)-Catalyzed Click Reaction-Triggered 3D DNA Walker for Constructing an "OFF−ON" Fluorescent Biosensor for Cu^{2+} Detection

Zhen Wang, Nan Jia, Xumei Zhou, Jing Han,* and Huaiyu Bu*

Cite This: *ACS Appl. Bio Mater.* 2021, 4, 3571−3578 Read Online

ACCESS | Metrics & More | Article Recommendations | Supporting Information

ABSTRACT: Herein, a highly selective and sensitive "OFF−ON" fluorescent biosensor was designed for intracellular Cu^{2+} detection. Compared to the fluorescent Cu^{2+} biosensors reported so far, this work tackled the tricky issue of reliability of Cu^{2+}, which mainly depends on the integration of the high selectivity of the Cu(I)-catalyzed click reaction with the ultrahigh sensitivity of a spherical nucleic acid-based 3D DNA walker. Typically, DNA track is carried out by coconjugating N_3-S1 and Cy3-HP onto gold nanoparticles (AuNPs). On this state, fluorophore (Cy3) was close to the surface of AuNPs (as a nanoquencher), generating a quenched fluorescence and thus causing the initial "OFF" state. In the presence of Cu^{2+} and H_2C_2-swing arm, Cu^+ was *in situ* generated quickly from the reduction of Cu^{2+} with the assistance of ascorbic acid, which could promptly and selectively trigger the Cu(I)-catalyzed click reaction-based 3D DNA walker between azide on N_3-S1 and alkyne on the H_2C_2-swing arm. Sequentially, the activated H_2C_2-swing arm was able to hybridize with adjacent Cy3-HP and the 3D DNA walker was automatically driven by N.BstNBI to produce multiple Cy3-labeled DNA fragments away from the AuNP surface for signal amplification, performing a recovered fluorescence response (turning into the "ON" state). Accordingly, the ingenious integration of an efficient click reaction and smart 3D DNA walker endows the constructed fluorescent biosensor with superior selectivity and ultrahigh sensitivity. We further apply this platform for Cu^{2+} sensing in biological systems; this assay will provide a signal transduction strategy for evaluating intracellular Cu^{2+} at picomolar levels.

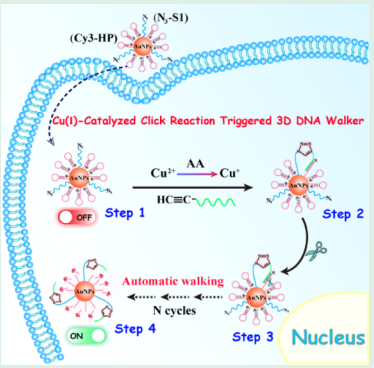

KEYWORDS: *fluorescent biosensor, click reaction, 3D DNA walker, signal amplification, Cu^{2+} detection*

INTRODUCTION

Copper ion (Cu^{2+}), as an essential micronutrient for living organisms, is closely related to enzyme regulation, metabolism, oxygen transport, and other biological processes.[1] However, abnormal levels of Cu^{2+} will interfere with cellular homeostasis and trigger aberrant oxidative damage, leading to liver or kidney damage and serious neurodegenerative diseases, such as Wilson's disease, Alzheimer's disease, and Menkes syndrome.[2] Therefore, exploiting simple, selective, and sensitive methods for Cu^{2+} detection in biological fluids and living cells is of great significance in the diagnosis and follow-up examination of relevant diseases. Currently, several reports of Cu^{2+} sensors were designed based on organic fluorescent probes,[3,4] peptides and proteins,[5,6] as well as nanomaterials.[7,8] However, some fluorescent sensing systems suffer from strong fluorescence quenching by the paramagnetic Cu^{2+} (*i.e.*, signal-off sensors) and are susceptible to interference from other metal ions (such as Co^{2+}, Ni^{2+}, Hg^{2+}, Pd^{2+}, and Fe^{3+}).[9,10] For Cu^{2+} sensing with organic probes, it also confronts with the predicaments of sophisticated synthesis and purification, and these probes usually react with Cu^{2+} at a ratio of 1:1; the detection limit is generally at the level of 10 nM.[11,12] More importantly, due to the complex cellular environments and the lack of effectiveness in the cell signal amplification manner, many of these assays still encounter the challenge of high selectivity and sensitivity of intracellular Cu^{2+} detection.

The Cu(I)-catalyzed alkyne−azide cycloaddition reaction, which owns the virtues of high ligation efficiency and specificity, can effectively improve the Cu^{2+} detection selectivity.[13−15] It is a typical five-membered triazole ring-forming reaction between azides and terminal alkynes with the catalysis of Cu^+ [Cu^+ can be generated from the reduction of Cu^{2+} in the presence of ascorbic acid (AA)]. Thus, it has become the gold standard of "click chemistry" and is widely used in nearly all areas of modern chemistry from drug discovery to materials science. However, research on Cu^{2+} biosensing by means of click chemistry is still in its infancy. Ge *et al.* proposed a colorimetric biosensor for visualizing the

Received: January 22, 2021
Accepted: March 13, 2021
Published: March 23, 2021

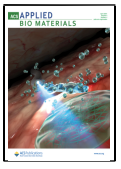

Scheme 1. Schematic Illustration of the Cu(I)-Catalyzed Click Reaction-Triggered 3D DNA Walker for Constructing the "OFF−ON" Fluorescent Biosensor for Intracellular Cu^{2+} Detection

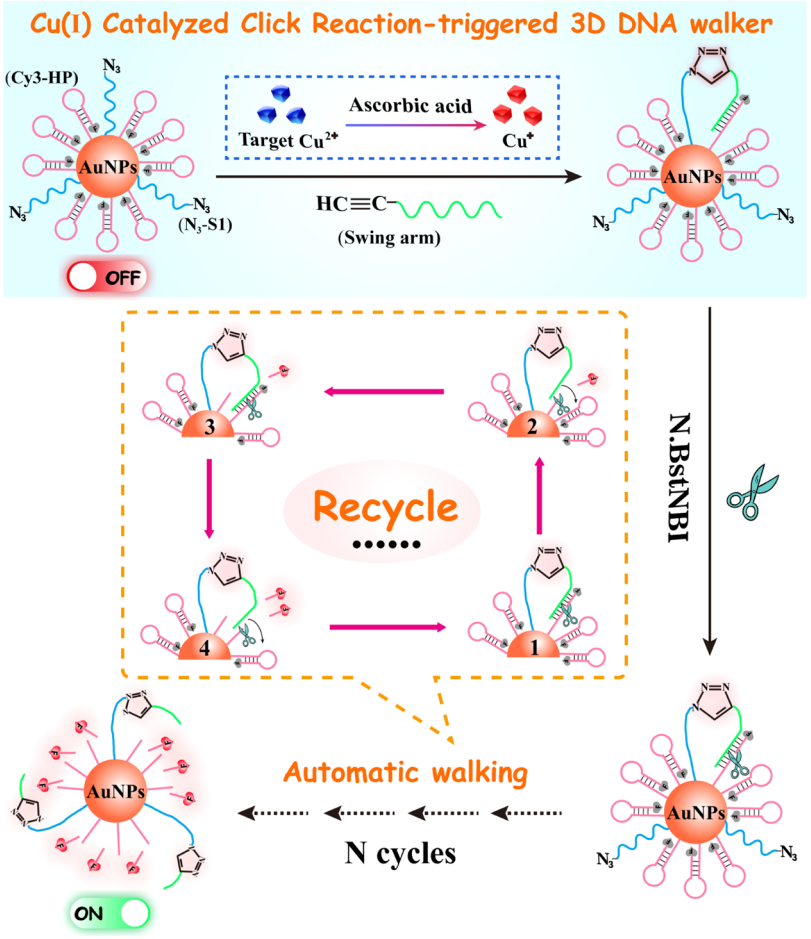

fluctuation of the Cu^{2+} concentration by engaging the click reaction as a bridge for the combination of hemin and G-quadruplex, and the limit of detection (LOD) is 100 nM.[16] Jiang's group developed a fluorescent method for Cu^{2+} detection on the basis of the click reaction and FRET (fluorescence resonance energy transfer) effect between graphene oxide and fluorescent dye; this GO-C_2&Rho-N_3 system can detect Cu^{2+} quickly and the LOD is evaluated to be 50 nM.[17] Aforementioned simple and elegant Cu^{2+} biosensors have greatly progressed the specificity and anti-interference ability, which prominently improves the reliability of Cu^{2+} monitoring. However, these assays still encounter the dilemma of relatively low detection sensitivity due to the failure to integrate signal amplification strategies. In fact, it is very difficult to incorporate signal amplification with most organic probe-based fluorescent biosensors. Accordingly, the exploration of a new fluorescent sensing platform that programs the signal amplification manner to improve the sensitivity of intracellular Cu^{2+} monitoring is compellingly needed.

DNA walker is viewed as a fantastically sensitive nucleic acid amplification tool that can convert chemical energy to mechanical motions and perform machine-like functions at the molecular level.[18,19] The autonomous movements of DNA walkers are typically based on a burnt-bridge mechanism in which sequential oligonucleotide hybridization is followed by toehold-mediated strand displacement or DNAzyme-/endonuclease-mediated hydrolysis of the fuel strand,[20−22] destructing the tracks and generating single-stranded products for signal amplification and target detection.[23−25] Previous studies have shown that the spherical nucleic acid (SNA)-based 3D DNA walker can accommodate hundreds of track strands, thus strikingly enhancing the local concentration of track DNA for improved walking efficiency and higher processivity, facilitating a high signal gain in a given period of time so as to improve the detection sensitivity, ascribing to the large surface-to-volume ratio of nanoparticles.[26] In this regard, the Cu(I)-catalyzed click reaction-based 3D DNA walker may be the most powerful technique for selective and sensitive Cu^{2+} detection. To the best of our knowledge, the intracellular Cu^{2+} monitoring based on the "OFF−ON" fluorescent biosensor using the SNA-based 3D DNA walker as the signal amplification pathway has not been reported.

Herein, we first proposed a 3D DNA walker directly triggered by the Cu(I)-catalyzed click reaction for intracellular Cu^{2+} detection. As shown in Scheme 1, the 3D track was constructed with N_3-S1 (azido-labeled) and Cy3-HP-functionalized gold nanoparticles (AuNPs). Meanwhile, the H_2C_2-swing arm was designed consisting of a walking strand with repeated T bases and a recognition site for the endonuclease (N.BstNBI) and containing an alkynyl group at the 3′ end for the click reaction. In the absence of Cu^{2+}, AuNPs could efficiently quench the fluorescence of surface-immobilized Cy3-HP because of the FRET from dye molecules (Cy3) to

https://doi.org/10.1021/acsabm.1c00073
ACS Appl. Bio Mater. 2021, 4, 3571−3578

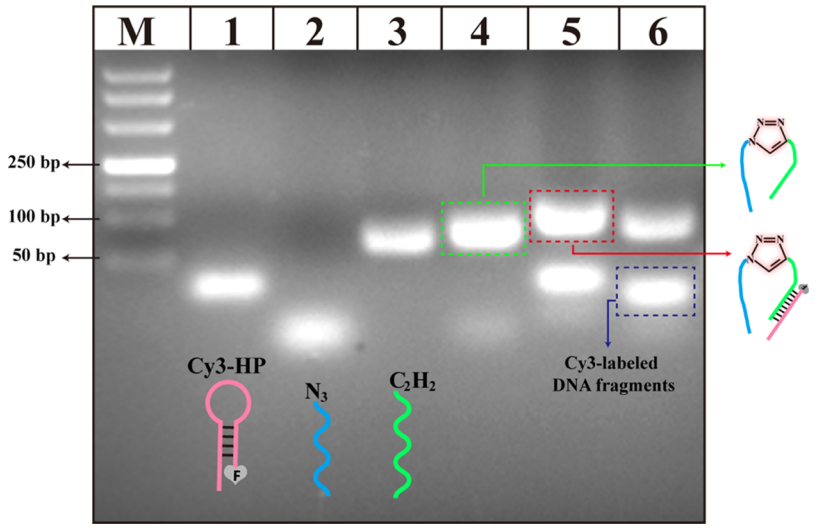

Figure 1. Agarose gel electrophoresis characterization for different samples: lane 1, Cy3-HP; lane 2, N_3-S1; lane 3, H_2C_2-swing arm; lane 4, the mixture of N_3-S1 and H_2C_2-swing arm with Cu^{2+} and AA; lane 5, the mixture of Cy3-HP, N_3-S1, H_2C_2-swing arm, Cu^{2+}, and AA; and lane 6, products of the Cu(I)-catalyzed click reaction-triggered 3D DNA walker.

the nanoquencher (AuNPs), leading to the initial "OFF" state. In the presence of Cu^{2+}, Cu^{+} was *in situ* generated from the reduction of Cu^{2+} with the assistance of AA. Synchronously, the 3D DNA walker was rapidly and selectively triggered due to the Cu(I)-catalyzed click reaction between azide on N_3-S1 and alkyne on the H_2C_2-swing arm. Sequentially, the activated H_2C_2-swing arm could bind and open the adjacent Cy3-HP and the 3D DNA walker was driven by N.BstNBI automatically, resulting in the release of multiple Cy3-labeled DNA fragments from the surface of AuNPs, thereby turning the system into the "ON" state and recovering the fluorescence response of Cy3 for signal amplification. Accordingly, the ingenious integration of the efficient Cu(I)-catalyzed click reaction and smart 3D DNA walker endows the constructed Cu^{2+} fluorescent biosensor with excellent selectivity and ultrahigh sensitivity. We further apply this platform for Cu^{2+} sensing in biological systems; this assay provides a new signal transduction strategy for evaluating intracellular Cu^{2+} at picomolar levels.

EXPERIMENTAL SECTION

Preparation of N_3-S1/Cy3-HP (DNA Track)-Functionalized AuNPs. The assembly of the DNA track was carried out by coconjugating N_3-S1 and Cy3-HP onto AuNPs. First, AuNPs with a diameter of 13 nm were prepared by reducing $HAuCl_4$ with sodium citrate following the literature protocol[27] (the detailed procedure is presented in the Supporting Information). For preventing disulfide formation, thiol-terminated N_3-S1 and Cy3-HP were pretreated with the TCEP solution (10 mM) in the dark for 40 min. Afterward, AuNPs, N_3-S1, and Cy3-HP were mixed at a molar ratio of 1:50:1000 and then left on a shaker to incubate overnight at room temperature. Tween 20 (1%) was then added to the mixture with a final concentration of 0.05% to prevent the adsorption and aggregation of AuNPs. Then, NaCl (1 M) was slowly added into the above solution over the next several hours in a "salt-aging" process, which reduces electrostatic repulsion between negatively charged neighboring oligonucleotide strands[28] and maximizes the oligonucleotide loading amounts,[29] as well as maintains the colloidal stability of AuNPs during the conjugation process. After incubation for an additional 24 h, the solution was centrifuged at 13,000 rpm for 20 min and washed twice with phosphate-buffered saline (PBS) (pH 7.4) to separate the N_3-S1/Cy3-HP-functionalized AuNPs from free DNA and unreacted reagents. Finally, the resulting colloid of N_3-S1/Cy3-HP-functionalized AuNPs was resuspended in PBS containing 0.05% Tween 20 and stored at 4 °C prior to use.

Agarose Gel Electrophoresis. Agarose gel (3%) was employed for the characterization of the different DNA oligonucleotides and the reaction products. Electrophoresis was performed in 1 × TBE buffer at 120 V for 30 min. The gel was imaged using the FUSION Solo6S (Vilber Lourmat Company Limited).

Cu(I)-Catalyzed Click Reaction-Triggered 3D DNA Walker for Cu^{2+} Detection *In Vitro*. A typical procedure for assaying Cu^{2+} is as follows: 20 μL of Cu^{2+} (different concentrations), 50 μL of the H_2C_2-swing arm (1 μM), and 5 μL of AA (10 mM) were incubated with 100 μL of the prepared N_3-S1/Cy3-HP-functionalized AuNPs at room temperature for 90 min. After that, the reacted solution was centrifuged at 13,000 rpm for 20 min and subsequently redispersed in the enzyme buffer (containing 10 μL of 10 × NEB and 1 μL of 10,000 U mL^{-1} N.BstNBI) at 55 °C for 60 min. Finally, the mixture was heated to 90 °C and kept for 10 min to deactivate the N.BstNBI. After cooling down to room temperature, the fluorescence intensity was monitored by an F-4500 fluorescence spectrophotometer with an excitation wavelength of 550 nm and an emission wavelength of 560 nm.

Cell Culture and Intracellular Imaging. Mouse macrophages (RAW264.7) were seeded in a 35 mm^2 glass-bottom cell culture dish and grown in Dulbecco's modified Eagle's medium supplemented with 100 U mL^{-1} penicillin, 100 U mL^{-1} streptomycin, and 10% fetal bovine serum. All cells were maintained at 37 °C in a humidified atmosphere of 5% CO_2 and 95% air. Before experiments, the adherent cells were washed with PBS and fixed with paraformaldehyde (4%) and then incubated with 20 μL of Cu^{2+} at 37 °C for 60 min. The cells were further incubated with a solution (containing N_3-S1/Cy3-HP-functionalized AuNPs, 50 μL of the H_2C_2-swing arm, 5 μL of AA, 10 μL of the 10 × NEB buffer, and 1 μL of N.BstNBI) different times. After washing three times with PBS, the fluorescence images of the cells were acquired under a confocal laser scanning microscope with an objective lens (60×) and 550 nm excitation.

RESULTS AND DISCUSSION

Principle of the Cu(I)-Catalyzed Click Reaction-Triggered 3D DNA Walker. The operating principle of the 3D DNA walker is illustrated in Scheme 1. The 3D track was constructed with SNA, which is based on 13 nm sized AuNPs functionalized with both thiol-tagged N_3-S1 and Cy3-HP *via* Au−S bonding. N_3-S1 was an azido-labeled single-strand DNA, as well as Cy3-HP was a self-hybridized hairpin probe with a

https://doi.org/10.1021/acsabm.1c00073
ACS Appl. Bio Mater. 2021, 4, 3571−3578

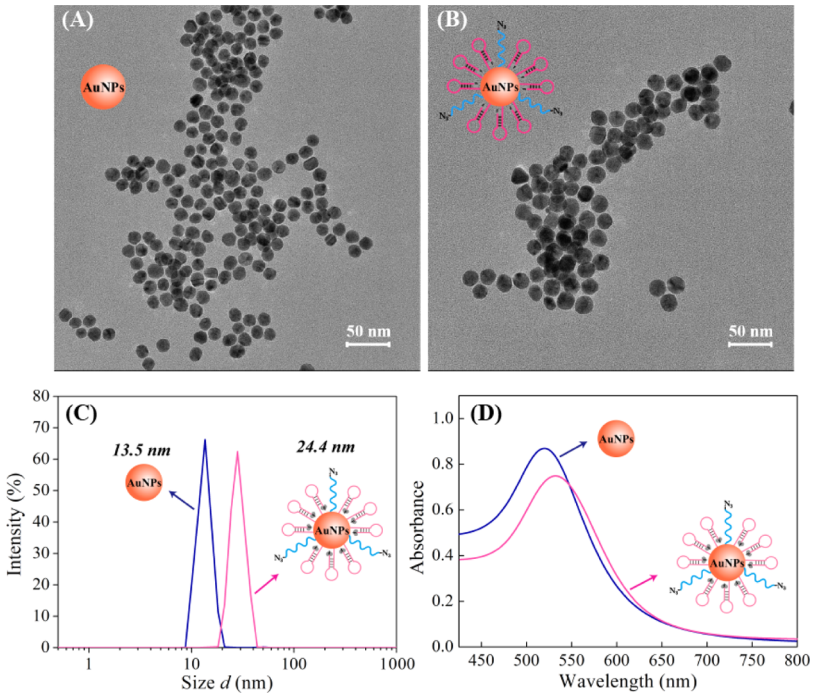

Figure 2. TEM images of (A) AuNPs and (B) N_3-S1/Cy3-HP-functionalized AuNPs. (C) DLS characterization and (D) UV−vis spectrum of AuNPs (blue curve) and N_3-S1/Cy3-HP-functionalized AuNPs (pink curve).

fluorescent group at the 5′ end as the signal output. Meanwhile, an alkynyl-labeled swing arm (H_2C_2-swing arm) was designed consisting of a walking strand with repeated T bases as the spacer and the complementary sequence for N.BstNBI recognition, as well as containing an alkynyl group at the 3′ end for the Cu(I)-catalyzed click reaction. In the absence of Cu^{2+}, AuNPs could efficiently quench the fluorescence of surface-immobilized Cy3-HP because of the FRET from dye molecules to the nanoquencher, leading to the initial "OFF" state. In the presence of Cu^{2+}, Cu^{+} was *in situ* generated from the reduction of Cu^{2+} with the assistance of AA. Synchronously, the 3D DNA walker was rapidly and selectively triggered due to the Cu(I)-catalyzed click reaction between azide on N_3-S1 and alkyne on the H_2C_2-swing arm. Thus, the H_2C_2-swing arm was activated and unfolded the prelocked Cy3-HP to form the recognition site for N.BstNBI (the asymmetric sequence 5′-GAGTC-3′ on Cy3-HP). Subsequently, N.BstNBI could identify and cleavage on the hybridized Cy3-HP, resulting in the release of Cy3-labeled DNA fragments from the surface of AuNPs so as to recover the fluorescence signal of Cy3 (turn into the "ON" state) and liberate the walking strand (H_2C_2-swing arm) as a free end again. Sequentially, the free walking strand was able to open the adjacent Cy3-HP to repeat the N.BstNBI nicking across the successive interface of AuNPs, yielding multiple Cy3 for signal amplification (the detailed sequence-related schematics is shown in Figure S1). Accordingly, the Cu(I)-catalyzed click reaction-triggered 3D DNA walker provides a new signal transduction platform for evaluating trace Cu^{2+} in biological systems with excellent selectivity and sensitivity.

Agarose Gel Electrophoresis Characterization. We conducted a preliminary agarose gel electrophoresis to verify the operation of the Cu(I)-catalyzed click reaction-triggered 3D DNA walker. In Figure 1, the bands of lanes 1, 2, and 3 represented hairpin Cy3-HP (40 nt), single-strand DNA of N_3-S1 (12 nt), and H_2C_2-swing arm (71 nt), respectively. Since DNA nucleotides of different molecular weights exhibited different migration velocities in electrophoresis, this accurately confirmed the identity of the three individual DNA oligonucleotides. Moreover, the formation of hairpin Cy3-HP can be further certified by IDT Oligo Analyzer calculations (the results are shown in Figure S2), which is mainly based on the value of Gibbs free energy to determine the probabilities that various hairpin structures may be formed in the case of the same nucleotide sequence. The values of Gibbs free energy for these six possible structures of Cy3-HP are in the following order: $\Delta G_1 < \Delta G_2 < \Delta G_3 < \Delta G_4 < \Delta G_5 < \Delta G_6$, indicating that structure (a) is the most easily formed, which is consistent with the principle of the experimental design. The mixture of N_3-S1, H_2C_2-swing arm, Cu^{2+}, and AA in lane 4 demonstrated that the ligation of N_3-S1 and the H_2C_2-swing arm was formed due to the Cu(I)-catalyzed click chemistry reaction between azide and alkyne groups; this was evidenced by the appearance of a band with a slightly increased molecular weight compared with lane 3. After the introduction of Cy3-HP, a clear band with a higher molecular weight in lane 5 further certificated the hybridization of the activated H_2C_2-swing arm with Cy3-HP. Subsequently, after cleaved by N.BstNBI, the Cy3-labeled DNA fragments (32 nt) with faster migration velocity can be observed in lane 6 (the number bases are in the middle between Cy3-HP and N_3-S1), liberating the walking strand (H_2C_2-swing arm) as the free end again. These results fully confirmed the Cu(I)-catalyzed click chemistry reaction-triggered 3D DNA walker, as well as the automatic operation by the specific cleavage of N.BstNBI, which provided a strong basis for the feasibility of the experimental progression.

Determination of N_3-S1/Cy3-HP (DNA Track) Loading on the AuNP Surface. The successful assembly of the DNA track on the surface of AuNPs is the first and crucial step before conducting the experiments, which is the prerequisite for the 3D DNA walker. The DNA track-AuNP conjugation was validated by transmission electron microscopy (TEM),

https://doi.org/10.1021/acsabm.1c00073
ACS Appl. Bio Mater. 2021, 4, 3571−3578

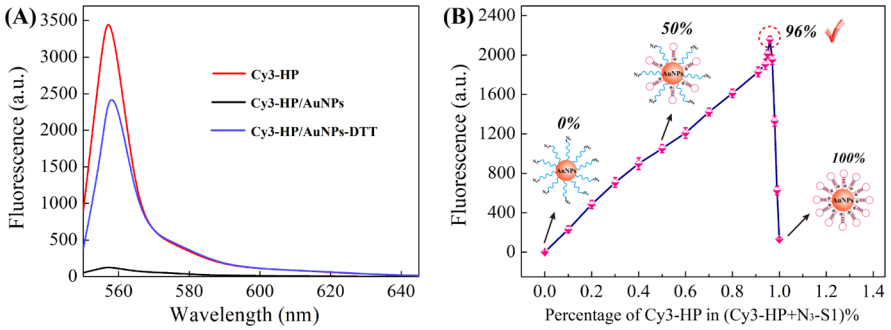

Figure 3. (A) Fluorescent spectrometry of Cy3-HP, Cy3-HP/AuNPs, and Cy3-HP/AuNPs-DTT. (B) Fluorescence measurements of the 3D DNA walker in the presence of Cu^{2+} and N.BstNBI at different proportions of Cy3-HP in the total of Cy3-HP and N_3-S1.

dynamic light scattering (DLS), and UV−vis spectrometry. As shown in Figure 2A, the typical TEM images of AuNPs exhibited a spherical shape with an average diameter of 13 nm, as well as confirmed the good dispersity of AuNPs before and after the surface coating of N_3-S1 and Cy3-HP, as shown in Figure 2B. DLS results further indicated that the hydrodynamic diameter of AuNPs changes from 13.5 to 24.4 nm after DNA conjugations (Figure 2C). Moreover, the red shift of the maximum absorption peak of N_3-S1/Cy3-HP-modified AuNPs in the UV−vis spectrum (Figure 2D) was observed and zeta potential analysis exhibited a more negative potential of N_3-S1/Cy3-HP-functionalized AuNPs compared to that of AuNPs (Figure S3), verifying the successful construction of N_3-S1/Cy3-HP-modified AuNPs.

The interaction between Cy3-HP and AuNPs was further determined by fluorescence measurements. As shown in Figure 3A, a high fluorescence signal was acquired when there was only Cy3-HP in the test buffer (red curve). However, the fluorescence intensity decreased sharply after the incubation with AuNPs (black curve), suggesting the fact that AuNPs as an efficient quencher could effectively quench the fluorescence of surface-immobilized Cy3-HP. Moreover, the fluorescence quenching efficiency of AuNPs with different particle sizes on Cy3 has been investigated (the results are presented in Figure S4). Subsequently, the conjugated Cy3-HP was detached from the surface of functionalized AuNPs using dithiothreitol (DTT) and further measured after centrifugation. Fluorescence intensity of the supernatant was approximately 72% of the original fluorescence value (blue curve), demonstrating that 72% of Cy3-HP was modified on the AuNPs successfully.

In order to evaluate the optional percentage of Cy3-HP in the total amount of loading DNA (Cy3-HP and N_3-S1) on AuNPs and assess the availability of the movement of the DNA machine, the fluorescence signals of the proposed biosensor were monitored in response to the target Cu^{2+}. As shown in Figure 3B, an improved fluorescence signal was observed for the activation of the 3D DNA walker in the presence of Cu^{2+} and N.BstNBI. As the proportion of Cy3-HP increased from 0 to 1, the fluorescence intensity enhanced steadily and reached the maximum at 96%, representing a strong DNA loading capability of AuNPs. Sequentially, the fluorescence values decreased dramatically with the increase of the ratio, indicating that Cy3-HP achieved the maximum amount for ensuring sufficient swing arms to operate the DNA walker.

Fluorescent Assay of Cu^{2+} *In Vitro*. Under optimal experimental conditions (the details are given in Figure S5), the Cu(I)-catalyzed click chemistry reaction-triggered 3D DNA walker for Cu^{2+} detection *in vitro* was investigated. The blank signal represented the fluorescence intensity of the biosensor without the addition of target Cu^{2+}, thus the 3D DNA walker would not be activated effectively, leading to a quenched fluorescence. With an incremental concentration of Cu^{2+} ranging from 0.1 pM to 10 nM, the corresponding fluorescence increased gradually, as observed in Figure 4. The

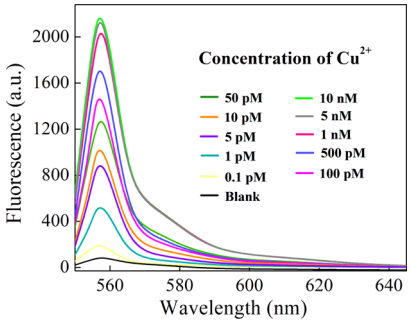

Figure 4. Quantitative detection of Cu^{2+} in the concentration range from 0.1 pM to 10 nM *in vitro* based on the 3D DNA walker.

inset in Figure S6 shows that it linearly responded to the logarithm of the Cu^{2+} concentration with a regression equation of $y = 422.9 \lg c + 612.3$ (y stands for the fluorescence intensity and c stands for the concentration of Cu^{2+}) and a squared correlation coefficient of $R^2 = 0.995$. The calibration curves in the inset suggested that the estimated LOD is 0.026 pM according to the principle of three times standard deviation (LOD = 3σ/slope, where σ is the standard deviation of the blank parallel determinations). The proposed Cu^{2+} fluorescent assay is highly sensitive compared with other various detection methods (Table S1), which critically depends on the integration of the Cu(I)-catalyzed click chemistry reaction-triggered and N.BstNBI-propelled 3D DNA walker.

Specificity, Stability, and Reproducibility for Cu^{2+} Assaying. To further assess the specificity of the Cu(I)-catalyzed click chemistry reaction-triggered 3D DNA walker, fluorescence responses of other metallic ions including Ca^{2+}, Mg^{2+}, Co^{2+}, Mn^{2+}, Ni^{2+}, Zn^{2+}, Fe^{3+}, and Ag^{+} were performed (the concentration of each interfering ion was 1 μM). As depicted in Figure 5, only the presence of Cu^{2+} (10 nM) resulted in a significant fluorescence. However, the addition of these interfering ions hardly caused obvious fluorescence signals even at high concentrations. Such comparison implied that the influence of other metallic cations toward Cu^{2+} detection is negligible. The excellent selectivity is attributed to the high specificity of the Cu(I)-catalyzed click chemistry reaction, which allows this method to be determined in

https://doi.org/10.1021/acsabm.1c00073
ACS Appl. Bio Mater. 2021, 4, 3571−3578

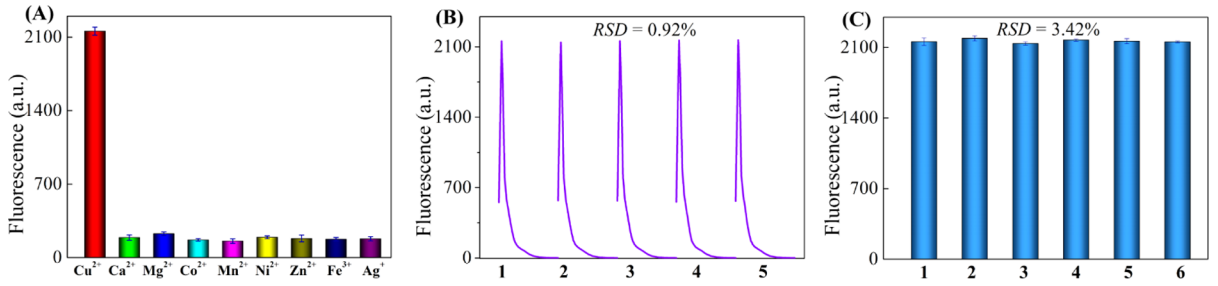

Figure 5. (A) Specificity of the proposed Cu^{2+} assay toward different interfering metallic ions. (B) Stability of the as-proposed biosensor incubated with 10 nM Cu^{2+} for intermittent fluorescence scanning. (C) Reproducibility was estimated by six differently prepared biosensors (incubated with 10 nM Cu^{2+}).

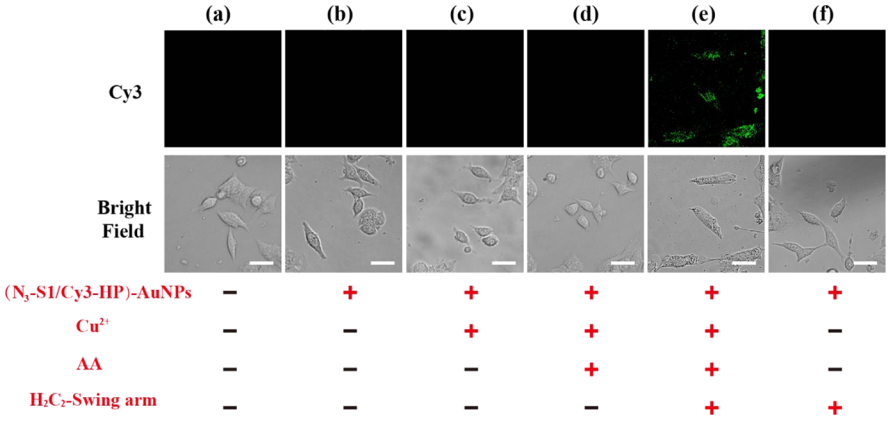

Figure 6. Confocal fluorescence images of mouse macrophages incubated with different probes: (a) normal mouse macrophage without probes. (b) (N_3-S1/Cy3-HP)-functionalized AuNPs. (c) Both (N_3-S1/Cy3-HP)-functionalized AuNPs and Cu^{2+}. (d) Mixed solution of (N_3-S1/Cy3-HP)-functionalized AuNPs, Cu^{2+}, and AA. (e) Mixture containing (N_3-S1/Cy3-HP)-functionalized AuNPs, Cu^{2+}, AA, and H_2C_2-swing arm. (f) Addition of (N_3-S1/Cy3-HP)-functionalized AuNPs and H_2C_2-swing arm but lack of Cu^{2+} and AA. Scale bar = 20 μm.

complex components without tedious pretreatment. Equally, stability and reproducibility are two significant criteria for evaluating the performance of the fluorescent biosensor. The intermittent fluorescence scanning repeated five times showed no obvious difference, as shown in Figure 5B, which indicates the acceptable stability of the proposed biosensor. The reproducibility was estimated by investigating six differently prepared biosensors with 10 nM Cu^{2+} (Figure 5C); the relative standard deviation was calculated to be 3.42%, revealing the prominent reproducibility of the proposed biosensor.

Intracellular Cu^{2+} Imaging. To test the application of the Cu(I)-catalyzed click reaction-triggered 3D DNA walker in a complex cellular environment, mouse macrophages were chosen as biological models for the cell uptake and Cu^{2+} imaging. First, the feasibility of the as-designed fluorescent biosensor for intracellular Cu^{2+} detection was elucidated by incubating macrophages with different probes. As shown in Figure 6a, macrophages exhibited the regular morphologies without any probes. Afterward, when treated with the preassembled N_3-S1/Cy3-HP-functionalized AuNPs, almost no apparent green emission from Cy3 was visible due to the FRET from Cy3 to the nanoquencher (AuNPs), generating a quenched fluorescence in Figure 6b. Later on, with the successive addition of target Cu^{2+} and AA (a reducing agent that quickly converts Cu^{2+} to Cu^{+}), fluorescence recovery was still not observed in Figure 6c,d. Obviously, upon the simultaneous introduction of (N_3-S1/Cy3-HP)-functionalized AuNPs, target Cu^{2+}, AA, and H_2C_2-swing arm, clear green emission was obtained from Figure 6e. Convincingly, in the presence of both Cu^{2+} and the H_2C_2-swing arm, Cu^{+} was *in situ* generated quickly from the reduction of Cu^{2+} with the assistance of AA, which could rapidly and selectively trigger the Cu(I)-catalyzed click reaction-based 3D DNA walker between azide on N_3-S1 and alkyne on the H_2C_2-swing arm. Sequentially, based on the automatic operation of the 3D DNA walker driven by N.BstNBI, multiple Cy3-labeled DNA fragments were detached away from the AuNP surface, performing a recovered fluorescence emission. To further demonstrate the key roles of Cu^{2+} and AA in the Cu(I)-catalyzed click reaction between N_3-S1 and the H_2C_2-swing arm, a comparative experiment is displayed in Figure 6f. Conceivably, no apparent fluorescence emission was observed because the click reaction could not be activated, which in turn verified the high selectivity and ligation efficiency of Cu(I)-catalyzed click chemistry.

To further investigate the fluorescence recovery as a function of the incubation time, the time-dependent fluorescence imaging experiments were recorded by cultured mouse macrophages with 6 μM Cu^{2+} for different timescales to monitor fluorescence emissions. As illustrated in Figure 7, faint fluorescence emission appeared after 15 min, which is due to the insufficient operation of the 3D DNA walker and release of Cy3-labeled DNA fragments within such a short time. Further extension of the incubation time to 60 min resulted in the gradually enhanced fluorescence emission. The results revealed the prominent specificity and the great potential of this platform for Cu^{2+} sensing, clearly indicating the practicability

https://doi.org/10.1021/acsabm.1c00073
ACS Appl. Bio Mater. 2021, 4, 3571−3578

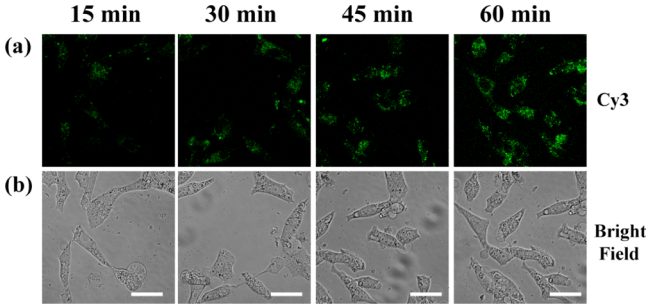

Figure 7. Confocal laser microscopic images of mouse macrophages that were incubated with 6 μM Cu^{2+} for different incubation times. Scale bar = 20 μm.

of our assay in intracellular Cu^{2+} imaging for the early screening of Cu-related metabolism diseases.

CONCLUSIONS

To summarize, we have established a highly selective and sensitive "OFF−ON" fluorescent biosensor for intracellular Cu^{2+} detection by coupling the Cu(I)-catalyzed click chemistry reaction-triggered and N.BstNBI-propelled 3D DNA walker. Compared to the fluorescent Cu^{2+} biosensors reported so far, the click chemistry-initiated DNA walker overcomes the restriction of low selectivity and anti-interference ability, which greatly tackles the critical issue of reliability of Cu^{2+} monitoring. The ultrahigh sensitivity can be principally attributed to the integration of N.BstNBI-assisted signal amplification strategies. Moreover, the proposed fluorescent biosensor was first applied for Cu^{2+} sensing in biological systems, providing a new concept on signal transduction for sensitive imaging of intracellular Cu^{2+}.

ASSOCIATED CONTENT

Supporting Information

The Supporting Information is available free of charge at https://pubs.acs.org/doi/10.1021/acsabm.1c00073.

Additional detailed sequence-related schematics of the fluorescent biosensor; six possible structures of Cy3-HP and the corresponding Gibbs free energy values; zeta potentials of bare AuNPs and N_3-S1/Cy3-HP-functionalized AuNPs; optimization of AuNPs with different sizes; and optimization of biosensing conditions (PDF)

AUTHOR INFORMATION

Corresponding Authors

Jing Han − *Key Laboratory of Synthetic and Natural Functional Molecule of the Ministry of Education, College of Chemistry & Materials Science, Northwest University, Xi'an, Shaanxi 710127, P. R. China;* orcid.org/0000-0001-8242-8200; Email: hanjing@nwu.edu.cn

Huaiyu Bu − *Shaanxi Provincial Key Laboratory of Biotechnology, Key Laboratory of Resource Biology and Biotechnology in Western China (Ministry of Education), Northwest University, Xi'an, Shaanxi 710069, PR China;* Email: buhy@nwu.edu.cn

Authors

Zhen Wang − *Key Laboratory of Synthetic and Natural Functional Molecule of the Ministry of Education, College of Chemistry & Materials Science, Northwest University, Xi'an, Shaanxi 710127, P. R. China*

Nan Jia − *Shaanxi Provincial Key Laboratory of Biotechnology, Key Laboratory of Resource Biology and Biotechnology in Western China (Ministry of Education), Northwest University, Xi'an, Shaanxi 710069, PR China*

Xumei Zhou − *Key Laboratory of Synthetic and Natural Functional Molecule of the Ministry of Education, College of Chemistry & Materials Science, Northwest University, Xi'an, Shaanxi 710127, P. R. China*

Complete contact information is available at: https://pubs.acs.org/10.1021/acsabm.1c00073

Notes

The authors declare no competing financial interest.

ACKNOWLEDGMENTS

We gratefully acknowledge the financial support from the NNSF of China (21973073 and 21973074) and the Natural Science Foundation of Shaanxi Province (2018JM2058).

REFERENCES

(1) Tripathy, S. K.; Woo, J. Y.; Han, C.-S. Surface-Plasmon-Based Colorimetric Detection of Cu(II) Ions Using Label-Free Gold Nanoparticles in Aqueous Thiosulfate Systems. *Nanotechnology* **2012**, *23*, 305502−305509.

(2) Que, E. L.; Domaille, D. W.; Chang, C. J. Metals in Neurobiology: Probing Their Chemistry and Biology with Molecular Imaging. *Chem. Rev.* **2008**, *108*, 1517−1549.

(3) Cotruvo, J. A., Jr.; Aron, A. T.; Ramos-Torres, K. M.; Chang, C. J. Synthetic Fluorescent Probes for Studying Copper in Biological Systems. *Chem. Soc. Rev.* **2015**, *44*, 4400−4414.

(4) Jo, J.; Lee, H. Y.; Liu, W.; Olasz, A.; Chen, C.-H.; Lee, D. Reactivity-Based Detection of Copper(II) Ion in Water: Oxidative Cyclization of Azoaromatics as Fluorescence Turn-On Signaling Mechanism. *J. Am. Chem. Soc.* **2012**, *134*, 16000−16007.

(5) Torrado, A.; Walkup, G. K.; Imperiali, B. Exploiting Polypeptide Motifs for the Design of Selective Cu(II) Ion Chemosensors. *J. Am. Chem. Soc.* **1998**, *120*, 609−610.

(6) Wegner, S. V.; Arslan, H.; Sunbul, M.; Yin, J.; He, C. Dynamic Copper(I) Imaging in Mammalian Cells with a Genetically Encoded Fluorescent Copper(I) Sensor. *J. Am. Chem. Soc.* **2010**, *132*, 2567−2569.

(7) Wang, J.; Pan, Y.; Jiang, L.; Liu, M.; Liu, F.; Jia, M.; Li, J.; Lai, Y. Photoelectrochemical Determination of Cu^{2+} Using a WO_3/CdS Heterojunction Photoanode. *ACS Appl. Mater. Interfaces* **2019**, *11*, 37541−37549.

(8) Zhao, X.-P.; Wang, S.-S.; Younis, M. R.; Xia, X.-H.; Wang, C. Asymmetric Nanochannel-Ionchannel Hybrid for Ultrasensitive and Label-Free Detection of Copper Ions in Blood. *Anal. Chem.* **2018**, *90*, 896−902.

(9) Wu, Q.; Anslyn, E. V. Catalytic Signal Amplification Using a Heck Reaction. An Example in the Fluorescence Sensing of Cu(II). *J. Am. Chem. Soc.* **2004**, *126*, 14682−14683.

(10) Lan, G.-Y.; Huang, C.-C.; Chang, H.-T. Silver Nanoclusters as Fluorescent Probes for Selective and Sensitive Detection of Copper Ions. *Chem. Commun.* **2010**, *46*, 1257−1259.

(11) Jung, H. S.; Kwon, P. S.; Lee, J. W.; Kim, J. I.; Hong, C. S.; Kim, J. W.; Yan, S.; Lee, J. Y.; Lee, J. H.; Joo, T.; Kim, J. S. Coumarin-Derived Cu^{2+}-Selective Fluorescence Sensor: Synthesis, Mechanisms, and Applications in Living Cells. *J. Am. Chem. Soc.* **2009**, *131*, 2008−2012.

(12) Si, H.; Sheng, R.; Li, Q.; Feng, J.; Li, L.; Tang, B. Highly Sensitive Fluorescence Imaging of Zn^{2+} and Cu^{2+} in Living Cells with Signal Amplification Based on Functional DNA Self-Assembly. *Anal. Chem.* **2018**, *90*, 8785−8792.

(13) Moses, J. E.; Moorhouse, A. D. The Growing Applications of Click Chemistry. *Chem. Soc. Rev.* **2007**, *36*, 1249−1262.

(14) Zhou, Q.-Y.; Yuan, F.; Zhang, X.-H.; Zhou, Y.-L.; Zhang, X.-X. Simultaneous Multiple Single Nucleotide Polymorphism Detection Based on Click Chemistry Combined with DNA-Encoded Probes. *Chem. Sci.* **2018**, *9*, 3335−3340.
(15) Qing, M.; Xie, S.; Cai, W.; Tang, D.; Tang, Y.; Zhang, J.; Yuan, R. Click Chemistry Reaction-Triggered 3D DNA Walking Machine for Sensitive Electrochemical Detection of Copper Ion. *Anal. Chem.* **2018**, *90*, 11439−11445.
(16) Ge, C.; Luo, Q.; Wang, D.; Zhao, S.; Liang, X.; Yu, L.; Xing, X.; Zeng, L. Colorimetric Detection of Copper(II) Ion Using Click Chemistry and Hemin/G-Quadruplex Horseradish Peroxidase-Mimicking DNAzyme. *Anal. Chem.* **2014**, *86*, 6387−6392.
(17) Zheng, W.; Li, H.; Chen, W.; Zhang, J.; Wang, N.; Guo, X.; Jiang, X. Rapid Detection of Copper in Biological Systems Using Click Chemistry. *Small* **2018**, *14*, 1703857.
(18) Feng, Q.-M.; Ma, P.; Cao, Q.-H.; Guo, Y.-H.; Xu, J.-J. An Aptamer-Binding DNA Walking Machine for Sensitive Electrochemiluminescence Detection of Tumor Exosomes. *Chem. Commun.* **2020**, *56*, 269−272.
(19) Chen, F.; Xue, J.; Bai, M.; Qin, J.; Zhao, Y. Programming in Situ Accelerated DNA Walkers in Diffusion-Limited Microenvironments. *Chem. Sci.* **2019**, *10*, 3103−3109.
(20) Tu, T.-T.; Lei, Y.-M.; Chai, Y.-Q.; Zhuo, Y.; Yuan, R. Organic Dots Embedded in Mesostructured Silica Xerogel as High-Performance ECL Emitters: Preparation and Application for MicroRNA-126 Detection. *ACS Appl. Mater. Interfaces* **2020**, *12*, 3945−3952.
(21) Bao, T.; Fu, R.; Wen, W.; Zhang, X.; Wang, S. Target-Driven Cascade-Amplified Release of Loads from DNA-Gated Metal-Organic Frameworks for Electrochemical Detection of Cancer Biomarker. *ACS Appl. Mater. Interfaces* **2020**, *12*, 2087−2094.
(22) Fu, Y.; Zou, K.; Liu, M.; Zhang, X.; Du, C.; Chen, J. Highly Selective and Sensitive Photoelectrochemical Sensing Platform for VEGF165 Assay Based on the Switching of Photocurrent Polarity of CdS QDs by Porous Cu_2O-CuO Flower. *Anal. Chem.* **2020**, *92*, 1189−1196.
(23) Liu, X.; Li, X.; Gao, X.; Ge, L.; Sun, X.; Li, F. A Universal Paper-Based Electrochemical Sensor for Zero-Background Assay of Diverse Biomarkers. *ACS Appl. Mater. Interfaces* **2019**, *11*, 15381−15388.
(24) Yang, X.; Tang, Y.; Mason, S. D.; Chen, J.; Li, F. Enzyme-Powered Three-Dimensional DNA Nanomachine for DNA Walking, Payload Release, and Biosensing. *ACS Nano* **2016**, *10*, 2324−2330.
(25) Zhang, K.; Yang, L.; Lu, F.; Wu, X.; Zhu, J.-J. A Universal Upconversion Sensing Platform for the Sensitive Detection of Tumour-Related ncRNA through an Exo III-Assisted Cycling Amplification Strategy. *Small* **2018**, *14*, 1703858.
(26) Cutler, J. I.; Auyeung, E.; Mirkin, C. A. Spherical Nucleic Acids. *J. Am. Chem. Soc.* **2012**, *134*, 1376−1391.
(27) Grabar, K. C.; Freeman, R. G.; Hommer, M. B.; Natan, M. J. Preparation and Characterization of Au Colloid Monolayers. *Anal. Chem.* **1995**, *67*, 735−743.
(28) Wang, S.; McGuirk, C. M.; Ross, M. B.; Wang, S.; Chen, P.; Xing, H.; Liu, Y.; Mirkin, C. A. General and Direct Method for Preparing Oligonucleotide-Functionalized Metal-Organic Framework Nanoparticles. *J. Am. Chem. Soc.* **2017**, *139*, 9827−9830.
(29) Cheng, Y. Y.; Xie, Y. F.; Li, C. M.; Li, Y. F.; Huang, C. Z. Förster Resonance Energy Transfer-Based Soft Nanoballs for Specific and Amplified Detection of MicroRNAs. *Anal. Chem.* **2019**, *91*, 11023−11029.

https://doi.org/10.1021/acsabm.1c00073
ACS Appl. Bio Mater. 2021, 4, 3571−3578